# btn1, the Schizosaccharomyces pombe homologue of the human Batten disease gene CLN3, regulates vacuole homeostasis

Yannick Gachet, Sandra Codlin, Jeremy S. Hyams, Sara E. Mole

# *btn1*, the *Schizosaccharomyces pombe* homologue of the human Batten disease gene *CLN3*, regulates vacuole homeostasis

**Yannick Gachet[1,*,‡], Sandra Codlin[2,§,‡], Jeremy S. Hyams[1,¶] and Sara E. Mole[1,2,§,**]**

[1]Department of Biology, University College London, Gower Street, London, WC1E 6BT, UK
[2]Department of Paediatrics and Child Health, University College London, Gower Street, London, WC1E 6BT, UK
*Present address: Institut d'Exploraton Fonctionelle des Génomes, Université Paul Sabatier, Toulouse 31062, France
‡These authors contributed equally to this work
§Present address: MRC Laboratory for Molecular Cell Biology, University College London, Gower Street, London, WC1E 6BT, UK
¶Present address: Institute of Molecular Biosciences, Massey University, Palmeston North 11222, New Zealand
**Author for correspondence (e-mail: s.mole@ucl.ac.uk)

*Accepted 16 August 2005*
*Journal of Cell Science 118, 5525-5536 Published by The Company of Biologists 2005*
*doi:10.1242/jcs.02656*

## Summary

**We have cloned the *Schizosaccharomyces pombe* homologue of the human Batten disease gene, *CLN3*. This gene, *btn1*, encodes a predicted transmembrane protein that is 30% identical and 48% similar to its human counterpart. Cells deleted for *btn1* were viable but had enlarged and more alkaline vacuoles. Conversely overexpression of Btn1p reduced both vacuole diameter and pH. Thus Btn1p regulates vacuole homeostasis. The vacuolar defects of *btn1Δ* cells were rescued by heterologous expression of CLN3, proving that Btn1p and CLN3 are functional homologues. The disease severity of Batten disease-causing mutations (G187A, E295K and V330F), when expressed in *btn1* appeared to correlate with their effect on vacuolar pH, suggesting that elevated lysosomal pH contributes to the disease process. In fission yeast, both Btn1p and CLN3 trafficked to the vacuole membrane via early endocytic and pre-vacuolar compartments, and localisation of Btn1p to the vacuole membrane was dependent on the Ras GTPase Ypt7p. Importantly, vacuoles in cells deleted for both *ypt7* and *btn1* were larger and more alkaline than those of cells deleted for *ypt7* alone, indicating that Btn1p has a functional role prior to reaching the vacuole. Consistently, *btn1* and *vma1*, the gene encoding subunit A of the V1 portion of vATPase, showed conditional synthetic lethality, and in cells deleted for *vma1* (a subunit of the vacuolar ATPase) Btn1p was essential for septum deposition during cytokinesis.**

Supplementary material available online at
http://jcs.biologists.org/cgi/content/full/118/23/5525/DC1

Key words: Btn1, CLN3, Juvenile neuronal ceroid lipofuscinosis, *Schizosaccharomyces pombe*, Vacuole

## Introduction

The neuronal ceroid lipofuscinoses (NCLs), also known as Batten disease, are a group of neurodegenerative diseases affecting children and characterised by the accumulation of autofluorescent material in the lysosomes of most cells (Santavuori, 1988). Clinical features include visual failure, seizures and progressive mental and motor deterioration leading to early death. The NCLs are inherited in an autosomal recessive manner and six human NCL genes have now been identified (International Batten Disease Consortium, 1995; Gao et al., 2002; Ranta et al., 1999; Savukoski et al., 1998; Sleat et al., 1997; Vesa et al., 1995; Vines et al., 1999; Wheeler et al., 2002). Despite a common cellular phenotype of disturbed lysosomal function, not all of the proteins causing NCL are located in this organelle (Heine et al., 2004; Isosomppi et al., 2002; Järvelä et al., 1999; Järvelä et al., 1998; Lonka et al., 2000; Lonka et al., 2004; Mole et al., 2004; Ranta et al., 2004).

Mutations in *CLN3* cause juvenile onset NCL (JNCL) that can be readily distinguished from the other NCLs (Goebel et al., 1999), and so far 39 mutations have been defined (see, http://www.ucl.ac.uk/ncl). *CLN3* encodes a 438 amino acid membrane protein that is glycosylated (Ezaki et al., 2003), phosphorylated (Michalewski et al., 1998; Michalewski et al., 1999) and probably farnesylated (Kaczmarski et al., 1999; Pullarkat et al., 1997). It is located in the endosome-lysosome membrane and in neuronal cells is additionally associated with synaptosomes and microvesicles (Ezaki et al., 2003; Haskell et al., 2000; Järvelä et al., 1999; Järvelä et al., 1998; Kyttälä et al., 2003; Luiro et al., 2001). Two targeting motifs for lysosomal location have been identified (Kyttälä et al., 2003; Kyttälä et al., 2005; Storch et al., 2004). CLN3 is predicted to be a transmembrane protein and probably spans the membrane six times with both termini projecting into the cytoplasm (Ezaki et al., 2003; Janes et al., 1996; Kyttälä et al., 2003; Mao et al., 2003).

The genes underlying two types of NCL (*CLN1/PPT1* and *CLN3*) are conserved in eukaryotes (Korey et al., 2003; Mitchell et al., 2001; Porter et al., 2005) including both budding yeast (*Saccharomyces cerevisiae, CLN3* only) (Pearce and Sherman, 1997) and fission yeast (*Schizosaccharomyces pombe*) (Cho et al., 2004) (this report). *CLN1* encodes the enzyme palmitoyl protein thioesterase 1 but the function of the

*CLN3* gene product, which has no homology with other proteins or functional domains, is unknown. However, its conservation suggests that it performs a fundamental cellular function. In budding yeast, Btn1p, the yeast orthologue of CLN3, is a vacuolar protein (the vacuole carrying out some of the functions of the lysosomes of higher eukaryotic cells) and has been implicated in vacuolar homeostasis (Pearce et al., 1999b; Pearce et al., 1998) although the molecular basis for this has not been determined. In cells deleted for Btn1p, decreased arginine transport into the vacuole (Kim et al., 2003), which is dependent on a functioning vATPase and vacuole acidification, has been reported, but this is at odds with the decreased vacuolar pH also reported in budding yeast cells missing functional Btn1p (Chattopadhyay et al., 2000; Pearce et al., 1999b).

The biology of *S. pombe* and *S. cerevisiae* are distinct in many respects, including the organisation of the vacuole (Moreno et al., 1991). Fission yeast has large numbers of small vacuoles (in the region of 50) (Bone et al., 1998) in contrast to budding yeast that contains a small number of large vacuoles. Fission yeast vacuoles fuse in response to hypotonic stress (Bone et al., 1998), a process dependent on the Ras GTPase Ypt7p (Bone et al., 1998). The fusion of isolated vacuoles from *S. cerevisiae* has been extensively studied (Seeley et al., 2002; Wickner, 2002) and many essential components for this and vesicle-mediated protein delivery to the vacuole in budding yeast are conserved in fission yeast (Takegawa et al., 2003). Since Batten disease is a lysosomal storage disease, we tested whether the fission yeast homologue of CLN3, Btn1p, was implicated in vacuole integrity and, if so, whether fission yeast was likely to provide a good model system for elucidating the basic function of Btn1p. The absence and overexpression of both wild-type and mutated *btn1* was shown to have significant effects on vacuole homeostasis and Btn1p also appeared to be functional in pre-vacuolar compartments. We therefore concluded that the use of fission yeast may prove to be pivotal in determining the function of both Btn1p and CLN3.

## Materials and Methods

### Identification of a *S. pombe* orthologue to CLN3

*btn1* was identified by searching the Sanger Centre Fission Yeast Genome Project (www.sanger.ac.uk/Projects/S_pombe) database for predicted proteins with homology to that encoded by the human disease gene, *CLN3* (U32680). The *btn1* gene resides on chromosome I, is contained in cosmid 607 (SPAC607.09c), and is retrievable from the EMBL database (accession number CAB63796). Sequences were aligned using ClustalX and shaded using MacBoxshade 2.15. The position of transmembrane domains are based on original predictions (Janes et al., 1996), recent work (Ezaki et al., 2003; Kyttälä et al., 2003; Mao et al., 2003) and the assumption that these will be conserved between mammalian and yeast species.

### *S. pombe* strains and cell growth

Strains used in this study are listed in Table 1. Media, growth, maintenance of strains and genetic methods were as described previously (Moreno et al., 1991). Cells were grown in rich medium (YES) or minimal medium (MM) containing appropriate supplements. For protein expression, cells were grown overnight in MM plus thiamine (4 μM). Cells were washed three times in MM lacking thiamine and grown for 18 hours in the same medium. Repression of the *nmt1* promoter (Maundrell, 1993) was carried out by the addition of 4 μM thiamine to log phase cells (usually $2\times10^6$ cells/ml). D-(–)-threo-2-amino-1-[p-nitrophenyl]-1,3-propainediol (ANP) was incorporated into MM agar at 1.0 mM.

### Gene deletion and construction of expression plasmids

The coding region of *btn1*$^+$ (all 396 amino acids plus the stop codon of the coding sequence) was replaced with the *leu2*$^+$ gene. A vector derived from pSL1180 was used to subclone the *leu2* gene (*Asc*I fragment) flanked by a 1 kb 5′ upstream region of *btn1* (amplified as a *Mlu*I-*Pst*I fragment using primers aaa acg cgt ttc ata atg atc cca tta ctg t and aac tgc aga aga ttc gta cta tat tta gta) and a 1.5 kb 3′ downstream region of *btn1* (amplified as a *Apa*I-*Nco*I fragment using primers aat tgg gcc caa aat agt gag tgc gca cat ct and cat gcc atg gca gca cca agc gaa aac cca). The plasmid (pSMr39) was linearised and transformed into a wild-type diploid strain. Transformants were selected for leucine auxotrophy, sporulated in MM without nitrogen and tetrads dissected using a Singer MSM Micromanipulator (Singer Instruments, Wachet, UK). Spores were inspected for growth on MM lacking leucine. Correct integration of the deletion cassette in selected colonies was confirmed by PCR using flanking primers to *btn1* and by Southern blotting of genomic DNA digested with *Eco*RI and probed with randomly primed radiolabelled *btn1* (see supplementary material, Fig. S1).

The *btn1* gene (1.2 kb) was subcloned into pREP1 (Maundrell, 1993) and pREP41GFP or pREP42GFP (Craven et al., 1998) as a *Sal*I-*Bam*HI fragment amplified from *S. pombe* genomic DNA using

**Table 1. Strains used in this study**

| Strain | Genotype | Source |
|---|---|---|
| Wild-type diploid | *ade210 ura4-D18, leu1-32/ade216 ura4-D18, leu1-32* | Laboratory stock |
| 972 | *h*$^-$ | Laboratory stock |
| ED665 | *h*$^-$, *ura4-D18, leu1-32, his2* | Laboratory stock |
| YG660 (btn1Δ) | *h*$^+$, *btn1::leu2, ura4-D18, leu1-32, his2* | This study |
| SC1 (btn1Δ) | *h*$^-$, *btn1::leu2, leu1-32* | This study |
| YG737 (YG660+pREP42GFPBtn1) | *h*$^+$, *ura4-D18, leu1-32, his2* | This study |
| SC12 (YG660+pREP42GFPBtn1$^{G136A}$) | *h*$^+$, *ura4-D18, leu1-32, his2* | This study |
| SC13 (YG660+pREP42GFPBtn1$^{E240K}$) | *h*$^+$, *ura4-D18, leu1-32, his2* | This study |
| SC14 (YG660+pREP42GFPBtn1$^{V278F}$) | *h*$^+$, *ura4-D18, leu1-32, his2* | This study |
| YG908 (YG660+pREP42GFPCLN3) | *h*$^+$, *ura4-D18, leu1-32, his2* | This study |
| ypt7Δ | *h*$^-$, *ypt7::ura4, ura4-D18, leu1-32* | J. Armstrong |
| YG434 (ypt7Δ+pREP41GFPBtn1) | *h*$^-$, *ypt7:: ura4, ura4-D18, leu1-32* | This study |
| YG904 (YG660+pREP42GFPYpt7) | *h*$^-$, *ypt7:: ura4, ura4-D18, leu1-32, his2* | This study |
| YG910 (ED665+pREP42GFPYpt7) | *h*$^+$, *ura4-D18, leu1-32, his2* | This study |
| SC2 (ypt7Δ btn1Δ) | *h*$^+$, *ypt7:: ura4, ura4-D18, btn1::leu2, leu1-32, his2* | This study |
| vma1Δ | *h*$^-$, *vma1::ura4, ura4-C190T, leu1-32* | K. Takegawa |
| SC3 (vma1Δ btn1Δ) | *h*$^-$, *vma1::ura4, ura4-C190T, btn1::leu2, leu1-32* | This study |
| vma3Δ | *h*$^-$, *vma3::ura4, ura4-C190T, leu1-32* | K. Takegawa |

primers 5′-acgcgtcgaccatgattaaattgaggttaac-3′ and 5′-cgggatcccgtcaagttaaggcacaccaat-3′, to allow expression from the *nmt* promoter. cDNA corresponding to the human *CLN3* gene was subcloned into pREP42GFP as a *Sal*I-*Bam*HI fragment using primers 5′-gtcgacaatgggaggctgtgcaggct-3′ and 5′-cgcggatccgcgtcaggagagctggcagagga-3′. *ypt7* was subcloned into pREP42GFP as a *Nde*I-*Bam*HI fragment amplified from *S. pombe* genomic DNA using primers 5′-gggaattccatatggccggcaaaaagaagca-3′ and 5′-cgcggatccgcgttaacagtaacatgaagtt-3′. Disease-causing mutations were introduced into clone pREP42GFPBtn1, which contained GFP fused to the N terminus of Btn1p, using the QuickChange site directed in vitro mutagenesis kit and following the manufacturer's instructions (Stratagene, La Jolla, CA, USA). Forward and reverse primers for each mutation are as follows: (i) human disease mutation G187A (GFPBtn1$^{G136A}$) 5′-tccggaacagccttggccggtctc-3′ and 5′-gagaccggcaaggctgttccgga-3′; (ii) mutation E295K (GFPBtn1$^{E240K}$) 5′-cttgtatacttctcaaaatatactatcaatattg-3′ and 5′-caatattgatagtatattttgagaagtatacaag-3′; (iii) mutation V330F (GFPBtn1$^{V278F}$) 5′-gtttaccagattggttttttcctatcgcgatc-3′ and 5′-gatcgcgataggaaaaaaccaatctggtaaac-3′. All constructs were verified by sequence analysis.

### Microscopy

For measurement of cell length and septation index, cells in log phase growth were fixed in 10% formaldehyde for 15 minutes, washed three times in 1× PBS and stored at 4°C. DNA was stained with DAPI, septa were visualised with calcofluor (Moreno et al., 1991) and cell length at division determined. For measurement of cell cycle length, exponentially growing cell were diluted to $0.5\times10^6$ cells/ml, a growth curve determined over 8 hours, and cell cycle length measured, as described previously (Alfa et al., 1993). FM4-64 dye (Molecular Probes) was used to label vacuoles if required. 1 μl FM4-64 (1 μg/μl in DMSO) was added to 1 ml cells. Cells were rotated at room temperature for 30 minutes, washed in MM and the dye incorporation chased for 30 minutes in MM. To monitor the rate of uptake of FM4-64 by endocytosis, 1 μl FM4-64 (1 μg/μl) was added to cells mounted in MM containing 1% agarose on a glass slide. To measure total fluorescent dye uptake, 6 μl of FM4-64 was added to 6 ml cells and incubated with agitation at 29°C. Uptake was arrested at the indicated time points by incubation at 0°C. A 1 ml aliquot of cells was washed with pre-cooled MM three times and the fluorescence was measured, at 620 nm, in triplicate samples of 200 μl each.

To monitor intravacuolar pH, 1 ml cells was stained with 1 μl carboxy-dichlorofluorescein diacetate (CDCFDA; 47 mM in DMSO; Molecular Probes) in 1 ml MM for 30 minutes, with rotation, at RT. Cells were washed three times in MM and incubated for 10 minutes in 1 ml MM, then placed on ice prior to viewing. To mark a subpopulation of cells prior to the start of the experiment, 1 ml of cells were pre-labelled with calcofluor and Hoechst stain (1 μl from stock solution) for 10 minutes, the cells were then washed three times in MM and mixed with 1 ml of a second population of cells marked only with calcofluor. All cells were exposed to 1 μl each of CDCFDA and FM4-64 and incubated for 15 minutes before observation. For quantitative CDCFDA hydrolysis, 6 ml exponentially growing cell were labelled with 10 μl of dye. The reaction was stopped after specified intervals by exposure to 0°C. A 1 ml aliquot of cells was washed with pre-cooled MM medium three times, and the fluorescence was measured at 520 nm in triplicate samples of 200 μl each. Measurement of CDCFDA against GFP (for relative pH measurements of Btn1p mutant proteins) was possible since the fluorescence of GFP was much lower than that of CDCFDA, such that GFP was not detectable at the short exposures needed for CDCFDA (0.01 seconds at 50% UV intensity), whereas detection of GFP needed an exposure of 1 second at full UV. Background fluorescence of GFP (even though effectively negligible) was subtracted where applicable.

Images were taken using either a Hamamatsu digital camera C4742-95 fitted to a Zeiss Axioskop microscope with plan-Apochromat 63× 1.4 NA oil immersion objective or a Hamamatsu C4742 CCD camera fitted to a Zeiss Axiophot microscope with a 64× 1.4 NA objective, and were recorded using OpenLab 3.15 software (Improvision Ltd., Coventry, UK), downloaded to Microsoft Excel for analysis and to Adobe Imageready 3 for assembly into montages. A FITC filter was used for CDCFDA detection.

### Visualisation, fusion and measurement of vacuoles

To visualise vacuoles, cells were labelled with 1 μl *N*-(3-triethylammoniumpropyl)-4-(6-(4-(diethylamino) phenyl) hexatrienyl) pyridinium dibromide (FM4-64) (Molecular Probes, 1 μg/ml in DMSO) with rotation for 30 minutes, washed in MM and then incubated for 30 minutes in MM. Vacuole fusion was assessed by labelling 1 ml log phase cells with FM4-64 for 30 minutes, which was then chased for 30 minutes. Cells were washed in $H_2O$ and resuspended in 1 ml $H_2O$ on ice for 2 hours, or overnight to ensure that full fusion had occurred. The diameter of every vacuole visible in one focal plane of a cell was measured using OpenLab 3.15 software and downloaded to Microsoft Excel for analysis (more than 300 vacuoles were counted for each data set). To determine the relationship between vacuole size and *btn1* expression, individual cells expressing GFP-Btn1 were assigned an expression level according to arbitrary units given by densitometry measurements, and 20 cells from each expression level were analysed for vacuole size. To correlate vacuole size with pH, cells were grown to log phase in MM. 10 ml cells were transferred to a small flask and labelled with FM4-64, as described. After the chase, 1 ml aliquots of the cells were placed into fresh Eppendorf tubes. Cells were pelleted and resuspended in MM combined with the appropriate pH buffer: 40 mM potassium hydrogen phthalate-HCl (pH range 3.5-4); 40 mM potassium hydrogen phthalate-NaOH (pH range 4.5-5.7); 40 mM potassium dihydrogen phosphate-dipotassium hydrogen phosphate (pH range 5.8-7.0) or 40 mM Hepes-NaOH (pH range 7.0-7.9), and grown for 1 hour. Vacuole size was determined at each pH value ($n$=100).

### pH determination

To calculate vacuole pH, 1 ml exponentially growing cells were exposed to 5 μl of LSDND/DND-189 (1 mM in DMSO; Molecular Probes) in MM + 40 mM Hepes pH 7.9 for 5 minutes at 25°C, and washed three times in MM. Quantitative fluorescence was determined using a Labsystem Fluoroskan Ascent FL microplate fluorometer with excitation at 450 nm and fluorescence reading at 520 nm for DND-189 (Cousin et al., 1997). Data from three independent experiments were exported to Excel for analysis. The vacuole pH was calculated from a standard curve, constructed by calibrating LSDND fluorescence against pH. Wild-type cells were loaded with LSDND, then permeabilised in the presence of bafilomycin (10 nM; Sigma), an inhibitor of vacuole ATPase, in 1 M sorbitol, 20% DMSO, 5 mM DTT 0.5% Triton X-100 for 4 minutes [protocol adapted from Li et al. (Li et al., 2000)] in the presence of buffers of different pH (50 mM sodium acetate pH 3.5, 3.8, 4; 50 mM MES pH 4.3, 4.58, 5, 5.5 and 6.15; 50 mM sodium phosphate pH 4.1 5, 5.6, 6, 6.5 and 7).

## Results

### Identification of a *S. pombe* orthologue of *CLN3*

The fission yeast homologue of *CLN3*, *btn1*, encodes a predicted transmembrane protein of 396 amino acids. Btn1p is 30% identical and 48% similar to its human counterpart (Fig. 1). Residues conserved between *S. pombe* Btn1p and vertebrate CLN3 proteins are also conserved in *S. cerevisae* Btn1p, notably in all proposed transmembrane segments as well as other regions including two of the predicted intra-organelle loops (CLN3 residues 161-211 and 304-370) and the C

terminus. Several regions conserved between vertebrate CLN3 proteins are absent in the yeast proteins (CLN3 residues 1-25; 65-92 inclusive) and residues in at least one of the motifs important for trafficking of CLN3 are conserved (CLN3 residues M409(X)$_9$G419). Amino acids affected by missense mutations that cause NCL (L101P, A158P, L170P, G187A, E295K, V330F, R334C, R334H, D416C) (see, http://www.ucl.ac.uk/ncl) are also conserved in *S. pombe* (L48, A106, L118, G136, E240, V278, R282, D363).

## Cells deleted for *btn1* have larger vacuoles

As a first step to determining the function of *btn1*, the gene was deleted by targeted replacement. Deletion of *btn1* was confirmed by Southern blotting of genomic DNA from transformants (supplementary material, Fig. S1A) and by PCR (not shown). Cells deleted for *btn1* (*btn1Δ*) were viable (Fig. 1B) albeit slower growing (Fig. 1C) and slightly longer at division (16±2.0 μm) than wild-type cells (13±1.7 μm) (Fig. 1B) when grown under normal laboratory conditions. *btn1Δ* cells also had a significantly higher septation index (13.1%) and an increase in the number of binucleate cells (6.3%) compared with wild type (8.6% septation, 2.2% binucleate) suggesting a perturbation of cell cycle progression. These pleiotropic effects could be complemented by reintroducing a plasmid containing the wild-type *btn1* gene fused at the N terminus with GFP (12.8±2.0 μm mitotic cell length, 8.0% septation and 2.6% binucleate), and human CLN3. Since Btn1p in budding yeast is a vacuolar protein we investigated vacuolar integrity in *btn1Δ* cells. Wild-type and *btn1Δ* cells were incubated in the dye FM4-64, which is taken up into fission yeast cells via the endocytic pathway (Brazer et al., 2000; Iwaki et al., 2004b) (Gachet and Hyams, 2005) eventually residing in the vacuoles, allowing their visualisation. Uptake of FM4-64 was similar in both wild-type and *btn1Δ* cells (supplementary material, Fig. S2A). Vacuoles in wild-type cells had a mean diameter of 0.92±0.26 μm whilst in *btn1Δ* the mean was 1.34±0.39 μm. This increase in vacuole size could be complemented by reintroducing a plasmid containing the human CLN3 gene fused at the N terminus with GFP (supplementary materials Fig. S2B). In both cases, vacuoles fused in response to hypotonic stress but in *btn1Δ* the fused vacuoles were again larger than those of wild-type cells (Fig. 2A,B). Cells lacking *btn1* had a larger total vacuolar volume than wild-type cells, both before and after fusion (data not shown).

## Cells deleted for *btn1* have more alkaline vacuoles

Vacuole size has recently been shown to relate to vacuolar pH (Iwaki et al., 2004a). We therefore investigated whether the increased vacuolar size in *btn1Δ* cells reflected increased vacuolar pH and whether the vacuole size was regulated in response to changes in external pH. We first monitored vacuolar pH using the proton sensitive probe CDCFDA which is membrane permeable until the acetate group is hydrolysed in the vacuole, whereupon it forms more highly charged compounds whose fluorescence intensity increases with

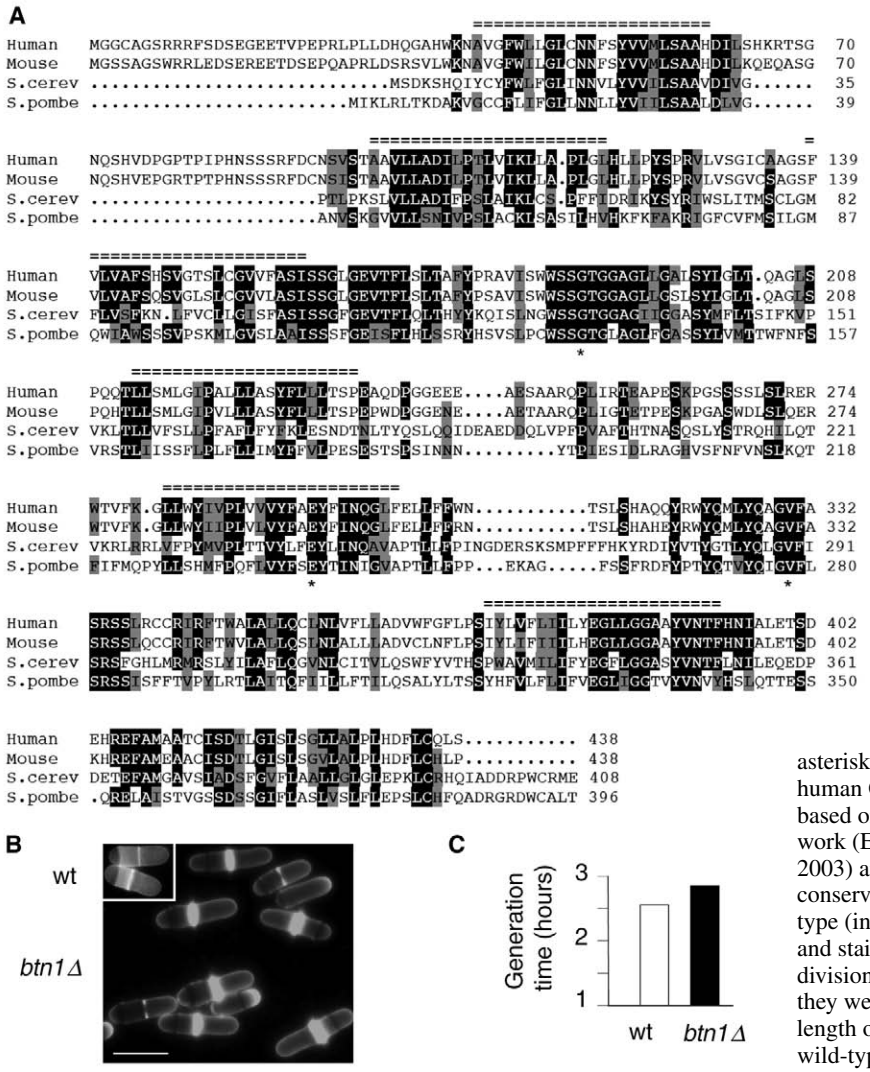


**Fig. 1.** Btn1p is the homologue of human CLN3. (A) Protein alignment between human CLN3 and its homologous proteins in mouse (Cln3) and two yeast species (Btn1), *S. cerevisiae* (S.cerev) and *S. pombe* (S.pombe). Shading indicates identical (dark) or similar (grey) residues. The position of residues mutated in *S. pombe* Btn1 during the course of this work that mimic those causing NCL are indicated by an asterisk (*). The likely transmembrane segments (TMS) in human CLN3 are indicated by ==. The position of TMS are based on original predictions (Janes et al., 1996), recent work (Ezaki et al., 2003; Kyttälä et al., 2003; Mao et al., 2003) and the assumption that the sequence of TMS will be conserved between mammalian and yeast species. (B) Wild-type (inset) and *btn1Δ* cells grown in YES medium at 29°C and stained with calcofluor. *btn1Δ* cells are longer at division (16±2.0 μm) than the wild-type cells from which they were derived (13±1.7 μm). Bar, 10 μm. (C) Cell-cycle length of *btn1Δ* cells (black bar) is increased compared to wild-type cells (white bar) at 29°C.

decreased vacuole pH (Pringle et al., 1989). *btn1Δ* cells had larger vacuoles and increased vacuolar pH (reduced CDCFDA fluorescence) than wild-type cells when grown in standard medium (Fig. 3A). *btn1Δ* cells were marked by staining nuclear DNA with Hoechst and then mixed with unstained wild-type cells, and vice versa (data not shown), to ensure that both strains were subjected to identical growth conditions. In both cases, calcofluor, which stains septa, was also used to show that similar fluorescence levels were observed in cells at different stages of the cell cycle. The size of vacuoles and their pH was clearly distinct between cells deleted for *btn1* and wild-type cells (Fig. 3B). The fluorescence intensity of CDCFDA increased linearly over time in both wild-type and *btn1Δ* cells (Fig. 3C). However, the intensity of fluorescence in *btn1Δ* cells was approximately 55% that of wild-type cells. This decrease could be rescued, at least partially, by reintroducing the *btn1* gene fused at the N terminus with GFP (Fig. 3C). We also used LSDND as an indicator of vacuolar pH since its fluorescence does not depend on uptake into the vacuole. The fluorescence intensity of LSDND increases as pH decreased (there is no fluorescence of LSDND at or above pH 6). Again *btn1Δ* cells had larger vacuoles and increased vacuole pH (reduced LSDND fluorescence) than wild-type cells (Fig. 3D). In *btn1Δ* cells, intravacuolar pH was estimated to be 5.1 in contrast to 4.14 in wild-type cells (Fig. 3E). *btn1Δ* cells also had increased sensitivity to growth on the chemical D-(–)-threo-2-amino-1-[p-nitrophenyl]-1,3-propainediol (ANP) (Pearce et al., 1999a), consistent with increased vacuole pH (supplementary material, Fig. S3).

Taken together, these results show that cells lacking functional Btn1p have larger and more alkaline vacuoles. We therefore investigated whether altered vacuolar pH was able to change vacuole size. Vacuole size and vacuole pH of wild-type and *btn1Δ* cells changed when exposed to media of different pH (pH 3.0-7.5) (Fig. 3F), presumably through a homeostatic mechanism to maintain the pH of the cytosol (Bone et al., 1998). Lower extracellular pH resulted in smaller vacuoles with increased CDCFDA fluorescence in both strains. Conversely, higher extracellular pH resulted in larger vacuoles and decreased CDCFDA fluorescence. Thus the vacuolar size defect of *btn1Δ* cells can be rescued by decreasing extracellular pH.

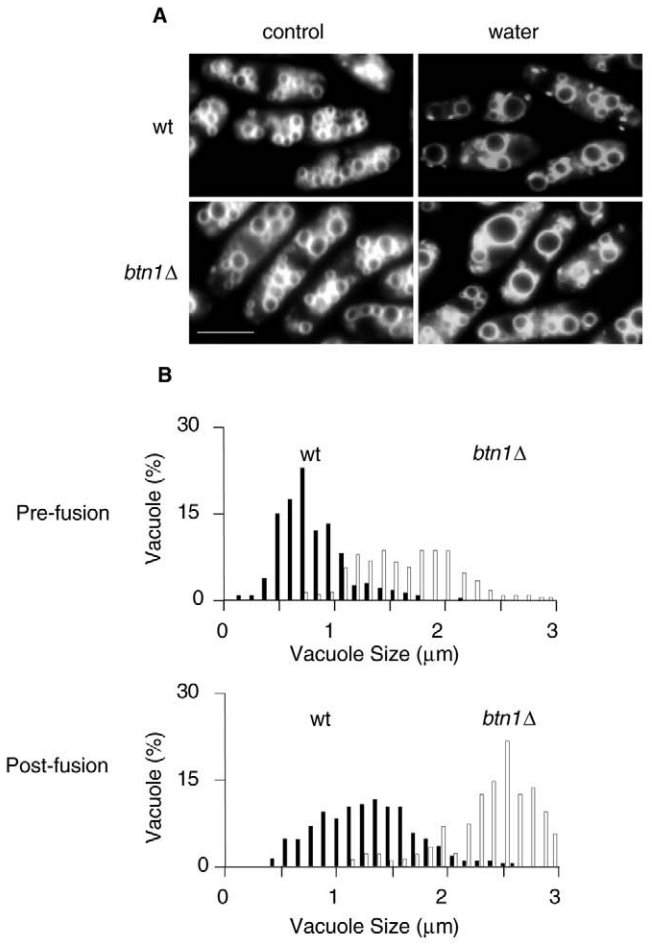


**Fig. 2.** *btn1Δ* cells have larger vacuoles. (A) Wild-type cells (top panels) and *btn1Δ* cells (lower panels) labelled with FM4-64 and observed by fluorescence microscopy during exponential growth (left panels) or hypotonic shock (right panels). Bar, 5 μm. (B) Vacuole size distribution before (upper panel) and after (lower panel) hypotonic shock in wild-type cells (black bars) and *btn1Δ* cells (white bars). Vacuole size is increased in *btn1Δ* cells before and after fusion in response to hypotonic shock.

## Btn1p traffics to the vacuole

Lack of functional Btn1p clearly affects the size and pH of the vacuole. We determined the location of Btn1p by introducing a wild-type *btn1* gene fused to GFP and under the control of the inducible *nmt42* promoter (Maundrell, 1993), into wild-type and *btn1Δ* deletion strains. This construct rescued the pleiotropic effects of *btn1Δ* cells (data not shown) as well as decreased intravacuolar pH (Fig. 3C). GFP-Btn1 localised to the vacuolar membrane (confirmed by pre-staining vacuoles with FM4-64) and to a variety of smaller, presumably pre-vacuolar compartments (Iwaki et al., 2004b) (Fig. 4A). To follow the trafficking of Btn1 and to identify its final location the *nmt42* promoter was repressed by the addition of thiamine. GFP-Btn1 was first visible in finger-like projections and cytoplasmic compartments mainly at the poles or septum of the cells, the major sites for endocytosis in *S. pombe* cells (Gachet and Hyams, 2005). These compartments co-stained early with FM4-64, consistent with a route that is identical or overlaps with an endocytic route via the plasma membrane (Fig. 4B). GFP-Btn1 was observed, over a 3-hour period, to traffic through theses small pre-vacuolar compartments to the vacuolar membrane (Fig. 4A).

## Over-expression of Btn1p decreases vacuolar size

To investigate whether Btn1 directly influenced vacuolar size, we expressed GFP-Btn1 in *btn1Δ* cells and correlated vacuolar size with the expression level of GFP-Btn1p by measuring the intensity of GFP fluorescence. We measured the size of vacuoles in cells with identical levels of GFP-Btn1 expression (Fig. 4C) and in cells following induction of GFP-Btn1 expression (Fig. 4D). Increasing Btn1p levels correlated with decreasing vacuolar size and, by extrapolation from earlier results, probably also with decreasing vacuolar pH.

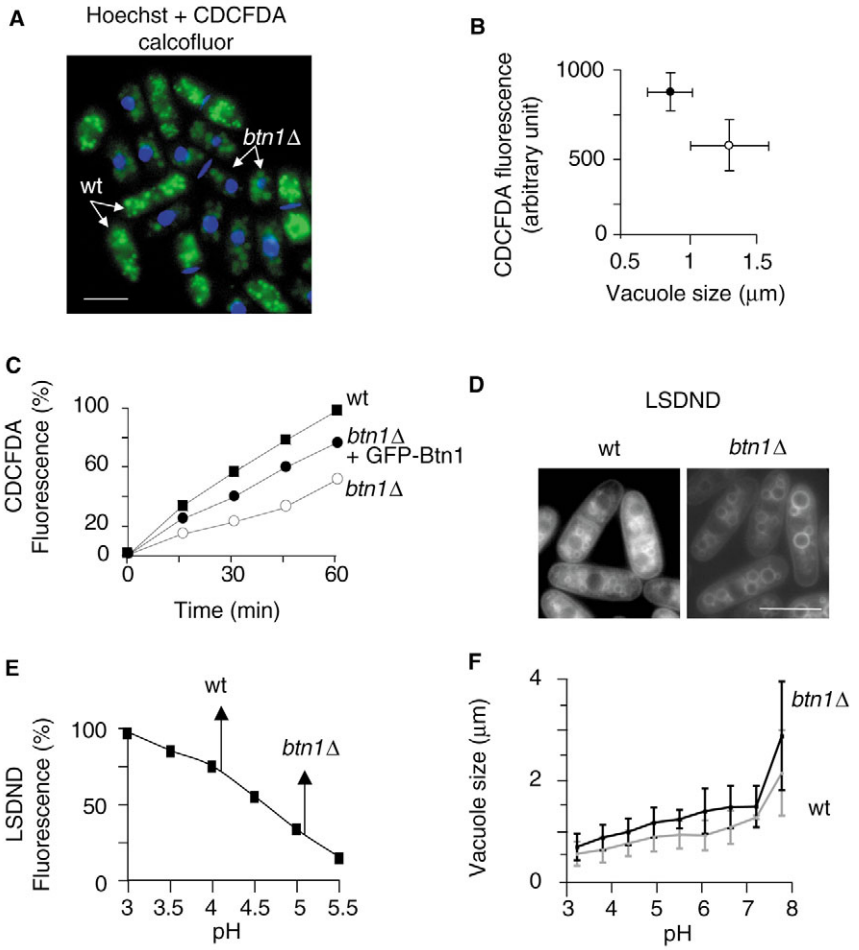


**Fig. 3.** Vacuoles of *btn1Δ* cells are more alkaline. (A) Cells deleted for *btn1* and prelabelled with Hoechst (blue) to stain nuclei and calcofluor (blue) to stain septa, were mixed with unlabelled wild-type cells, also prelabelled with calcofluor (blue), and incubated with CDCFDA (green, to indicate relative intravacuolar pH) for 10 minutes. A wild-type and a *btn1Δ* cell (distinguished by round nuclear staining) are indicated by arrows. Vacuoles in *btn1Δ* cell had reduced CDCFDA fluorescence indicating an increased pH. Bar, 10 μm. (B) Correlation between CDCFDA fluorescence and vacuole size for cells deleted for *btn1Δ* (open circles) and wild-type cells (filled circles). (C) Time course of hydrolysis of CDCFDA as an indicator of relative intravacuolar pH and measured by quantitative fluorescence in wild-type cells (filled squares), cells deleted for *btn1* (open circle) or cells deleted for *btn1* and expressing GFP-Btn1 for 18 hours (filled circles). GFP-Btn1 partially rescues the reduced CDCFDA fluorescence of *btn1Δ* cells. (D) Wild-type cells (left panel) and *btn1Δ* cells (right panel) labelled with LSDND as an indicator of relative vacuole pH. Note that *btn1Δ* cells have reduced fluorescence. Bar, 10 μm. (E) Vacuole pH estimation of wild-type and *btn1Δ* cells. The vacuoles of *btn1Δ* cells are pH 5.1 compared to those in wild-type cells which are 4.14. (F) Mean vacuole diameter of wild-type and *btn1Δ* cells exposed to media of different pH. The vacuole diameter of both strains increased as cells were exposed to media of increasing pH.

### *btn1* and *vma1* show conditional synthetic lethality

The major contributor to the acidic pH of the vacuole is the activity of the vacuolar ATPase complex (vATPase) (Mellman et al., 1986; Takegawa et al., 2003; Iwaki et al., 2004a). *S. pombe* cells deleted for subunits of vATPase (Iwaki et al., 2004a) have extremely large, alkaline vacuoles and significantly reduced endocytosis. Surprisingly, GFP-Btn1p trafficked directly to the vacuole membrane in cells deleted for *vma1* (or *vma3*, unpublished data), the gene encoding subunit A of the V1 portion of vATPase, and caused a striking reduction in vacuole size (supplementary material, Fig. S4A). This suggests that Btn1p can utilise a second trafficking route to the vacuole that bypasses the endocytic pathway. Since Btn1p and vATPase affect vacuole pH we examined the effect of combining *btn1Δ* and *vma1Δ* deletions. *btn1Δvma1Δ* cells were viable at 25°C and there was no difference in vacuole pH or ability to grow on media of varying pH between cells lacking *vma1* or cells lacking *vma1* and *btn1* (supplementary material, Fig. S4B). However, Btn1 protein was essential for survival at any temperature over 30°C (Fig. 5A). After incubation for 2 hours at 30°C, 86% of *btn1Δvma1Δ* cells were binucleate and showed no septum deposition, and after 4 hours at the non-permissive temperature, 98% of cells were elongated and multinucleated without any septum deposition (Fig. 5B) compared to *vma1Δ* cells (6%) or *btn1Δ* cells (8.2%). Thus at higher temperatures, cells deleted for both *btn1* and *vma1* were elongated and swollen, and unable to initiate septum deposition, suggesting a severe defect in cytokinesis.

### Trafficking of Btn1p to the vacuole is Ypt7 dependent

The Rab GTPase Ypt7p is essential for heterotypic (vesicle-) and homotypic (vacuole-) vacuole fusion in *S. pombe* (Bone et al., 1998; Iwaki et al., 2004b; Murray et al., 2001). GFP-Btn1 failed to localise to the small vacuoles of *ypt7Δ* cells (as defined by FM4-64 staining) but was retained in pre-vacuolar compartments (defined by lack of FM4-64 staining following its chase to vacuoles; Fig. 6A) indicating that Btn1p requires Ypt7p-dependent heterotypic fusion to traffic to the vacuole, consistent with our earlier observations on trafficking routes of Btn1p. However, GFP-Ypt7 localised correctly in *btn1Δ* cells (supplementary material, Fig. S5) and vacuoles were enlarged when GFP-Ypt7 was overexpressed in both wild-type and *btn1Δ* cells, suggesting that overexpression of Ypt7p increased vacuole fusion and overrode the effect of deleting *btn1*. Cells lacking *ypt7* have smaller vacuoles (0.39±0.13 μm) than wild-type cells (Fig. 6A-C) because of the intrinsic defect in fusion. Just as deleting *btn1* from wild-type cells resulted in larger vacuoles (1.34±0.39 μm; Fig. 2A,B), so the vacuoles of cells lacking both *ypt7* and *btn1* were larger than those of *ypt7* cells (0.68±0.18 μm; Fig. 6B,C). The vacuoles of cells lacking *ypt7* or *ypt7* and *btn1* did not fuse in response to hypotonic shock (Fig. 6B). In addition the fluorescence of CDCFDA in vacuoles

was more intense in *ypt7Δ* cells than in cells lacking both *ypt7* and *btn1* (Fig. 6D), consistent with *ypt7Δbtn1Δ* cells having more alkaline vacuoles than *ypt7* cells. This indicates that in cells deleted for *ypt7* only, Btn1p was affecting vacuole size and pH from its location in the prevacuolar compartment. These results support a functional role in a pre-vacuolar compartment for Btn1p. Finally *ypt7* and *btn1* showed conditional synthetic lethality at 30°C (data not shown).

## The human *CLN3* gene can functionally compensate for *btn1*

We determined the intracellular location of CLN3 fused to GFP. Heterologous expression of this chimeric protein resulted in rapid trafficking of GFP-CLN3 to the vacuole membrane, such that immediately following promoter repression all GFP-CLN3 was present in the vacuole (Fig. 7A). Thus Btn1p and CLN3 both traffic to the vacuole, albeit with different kinetics. We examined whether Btn1p and CLN3 could restore the vacuolar sise and pH defects of *btn1Δ* cells. Overproduction of both GFP-Btn1 and GFP-CLN3 protein resulted in a reduced vacuole size (Fig. 7B,C) and also decreased pH (Fig. 7C) as monitored by increased CDCFDA fluorescence. Thus, CLN3 can functionally compensate for lack of Btn1 in terms of defects in vacuolar pH and size.

## Effect of CLN3 disease mutations on vacuole homeostasis

Since CLN3 can substitute for Btn1p, we investigated whether mutations in Btn1p, which mimicked those in CLN3 causing human disease, affected its intracellular location and vacuolar function. There are ten missense mutations in CLN3 (see, http://www.ucl.ac.uk/ncl) that change conserved amino acid residues, most of which cause classic JNCL disease. However, some result in an altered disease course (Munroe et al., 1997) suggesting that the mutant protein retains some residual function. We first examined the location of three GFP-Btn1 proteins carrying different missense mutations 3 hours after repression of their expression in *btn1Δ* cells. GFP-Btn1$^{G136A}$ (CLN3 mutation G187A) was retarded in the endoplasmic reticulum (Pidoux et al., 1993) whereas GFP-Btn1$^{E240K}$ (E295K) and GFP-Btn1$^{V278F}$ (V330F) trafficked to the vacuolar membrane through the prevacuolar compartments (Fig. 7D), although slightly more slowly that wild-type Btn1. We next examined the effect of expressing these mutations on the vacuolar size of *btn1Δ* cells. The vacuoles of cells expressing all three mutant proteins remained enlarged in contrast to those expressing wild-type Btn1, which were reduced in size (Fig. 7B). Cells overexpressing GFP-Btn1$^{E240K}$ were also strikingly elongated (mean cell length at division was 22.1 μm) with an increased number of binucleate cells (10.5%) and increased septation index (19.0%) (Fig. 7D) suggesting a significant perturbation in the cell cycle. Cell length at mitosis and duration of septation of cells expressing GFP-Btn1$^{G136A}$ and GFP-Btn1$^{V278F}$ did not differ significantly from cells lacking the *btn1* gene, although the number of binucleate cells was slightly increased (7.9% for GFP-

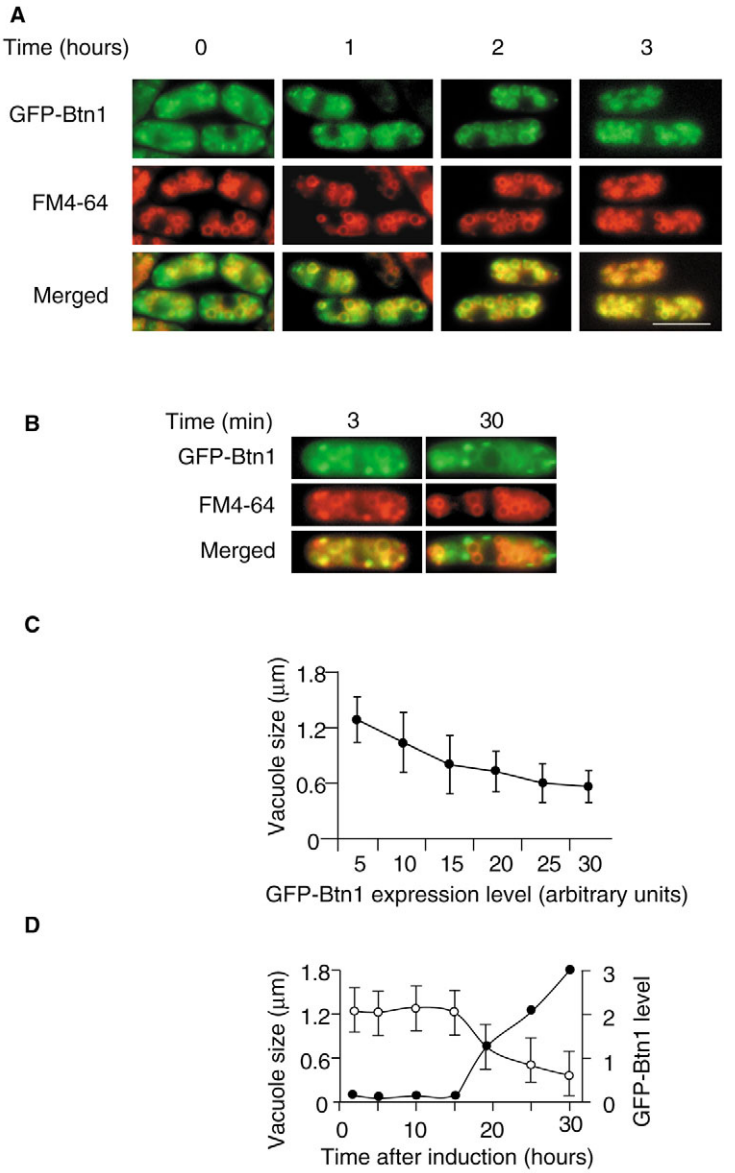


**Fig. 4.** Localisation and effect of overexpressed Btn1p. (A) Cells deleted for *btn1* and expressing GFP-Btn1 for 18 hours (green, left top panel) were labelled with FM4-64 (red, left middle panel) to show the steady state location of GFP-Btn1. At time 0 the promoter *nmt42* was repressed by the addition of thiamine and the location of GFP-Btn1 followed and compared with FM4-64 staining of vacuoles at hourly intervals. GFP-Btn1 was first visible in compartments adjacent to the poles or septum of the cells, then over a 3-hour period trafficked through these small pre-vacuolar compartments to the vacuolar membrane. Bar, 10 μm. (B) In cells deleted for *btn1* and expressing GFP-Btn1 (green, top panel), the uptake of FM4-64 after 3 minutes and 30 minutes (red, middle panel) was compared with the location of GFP-Btn1. GFP-Btn1 colocalised with compartments that were stained with FM4-64, indicating trafficking through the endocytic route. (C) Correlation of vacuole size with GFP-Btn1 expression levels in *btn1Δ* cells. Vacuoles were visualised by FM4-64 staining and GFP expression by densitometry. Cells having the highest levels of expression of GFP-Btn1 had the smallest vacuoles, and vice versa. (D) Time course of vacuole size and GFP-Btn1 expression in *btn1Δ* cells. Vacuole size (open circles) was visualised by FM4-64 staining and GFP expression (filled circles) by fluorimetry. As overall levels of GFP-Btn1 increased following induction of expression, the average vacuolar size decreased.

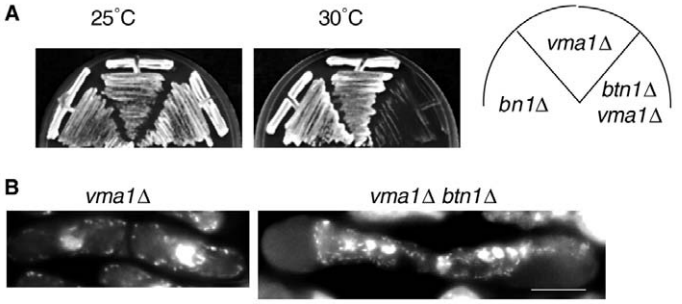


**Fig. 5.** *btn1* and *vma1* show conditional synthetic lethality. (A) *btn1Δvma1Δ* cells were viable at 25°C but Btn1 protein was essential for survival at 30°C. (B) DAPI and calcofluor staining of cells deleted for *vma1* and *btn1vma1* at 36°C. *btn1Δvma1Δ* cells were unable to initiate septum formation and many were elongated. Bar, 10 μm.

Btn1$^{G136A}$ and 8.2% for GFP-Btn1$^{V278F}$). We then monitored CDCFDA fluorescence to compare the vacuolar pH of the mutants expressed in *btn1Δ* cells (Fig. 7C). For GFP-Btn1$^{G136A}$, vacuolar pH was similar to that in *btn1Δ* cells. For GFP-Btn1$^{E240K}$ and GFP-Btn1$^{V278F}$, the pH defect was partially rescued (Fig. 7C), though not as well as by wild-type Btn1 or CLN3 protein. Thus, mutant Btn1p protein that can traffic to the vacuole may be capable of restoring vacuole pH but not vacuole size. In addition, in fission yeast it appears that control of vacuole size and pH regulation can be dissociated.

## Discussion

### Btn1p is the functional homologue of CLN3

We identified *btn1*, the fission yeast homologue of the human Batten disease gene, *CLN3*, on the basis of sequence homology and functional complementation of a *btn1* null strain by heterologously expressed CLN3. Many residues are conserved between vertebrate and fungal species, suggesting that these are critical to structure and/or function. These include residues important for trafficking of CLN3 (Kyttälä et al., 2003) and those affected by missense mutations (see, http://www.ucl.ac.uk/ncl). Other regions are absent or reduced in lower organisms, suggesting that these are not critical for function in these species. Btn1p is predicted to be a transmembrane protein and a GFP-Btn1 fusion protein localised to the vacuole membrane and to various pre-vacuolar compartments, in agreement with the observed location of CLN3 (Ezaki et al., 2003; Haskell et al., 2000; Järvelä et al., 1999; Järvelä et al., 1998; Luiro et al., 2001). Promoter repression experiments resulted in the accumulation of the fusion protein exclusively in the vacuole membrane, which we concluded was the final destination of Btn1p. In budding yeast, overexpression of its CLN3 homologue gave a location either in the matrix or in the membrane of the vacuole (Croopnick et al., 1998). The fission yeast *btn1* null strain is viable but has vacuolar defects that are rescued by GFP-Btn1p and GFP-CLN3 chimeras, consistent with their location, and shows subtle and reproducible defects in cell cycle progression (both G2 and cytokinesis are extended) that are probably secondary effects. We are confident therefore that we have correctly identified the cellular location of Btn1p. A vacuole location for Btn1p, or an effect on vacuole function, is consistent with accumulation of storage of material in the lysosome in the human disease. However, since trafficking of GFP-Btn1 to the vacuole took significantly longer than that reported for other vacuolar membrane proteins in *S. pombe* (Bellemare et al., 2002; Gaits et al., 1999; Iwaki et al., 2003), Btn1p may be specifically retarded in its trafficking and exerting a functional effect en route to the vacuole.

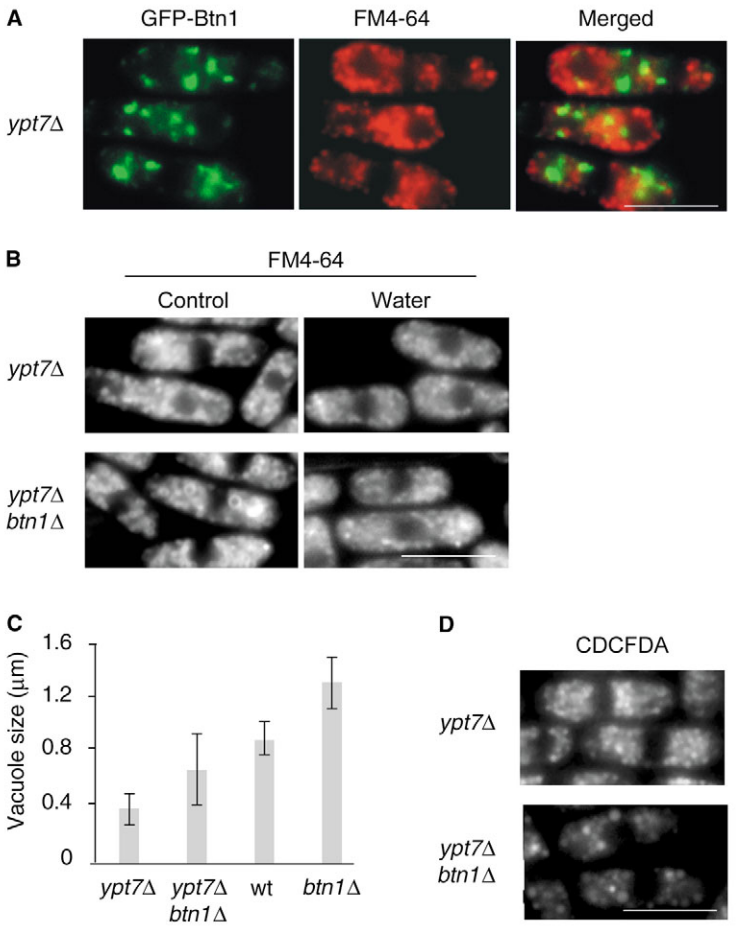


**Fig. 6.** Trafficking of Btn1p to the vacuole is Ypt7 dependent. (A) Localisation of GFP-Btn1 (green, left panel) in cells deleted for *ypt7* and pre-labelled with FM4-64 (red, middle panel). GFP-Btn1 does not traffic to the vacuole in *ypt7Δ* cells. Bar, 10 μm. (B) Cells deleted for *ypt7* or for *ypt7* and *btn1* were incubated with FM4-64 for 2 hours (left panel) then submitted to hypotonic shock (right panel). Vacuoles of *ypt7Δ cells* were smaller than those of cells deleted for *ypt7* and *btn1*, and vacuoles of both strains were unable to fuse in response to hypotonic shock. Bar, 10 μm. (C) Vacuole size analysis in wild-type (wt) and cells deleted for *btn1*, *ypt7* or *ypt7* and *btn1*. Absence of Btn1p in *ypt7Δ* cells resulted in larger vacuoles. (D) Cells were incubated with CDCFDA for 10 minutes, to indicate relative intravacuolar pH. Cells deleted for *ypt7* and *btn1* had reduced CDCFDA fluorescence, indicating vacuoles were more alkaline than those of cells deleted for *ypt7*. Bar, 10 μm.

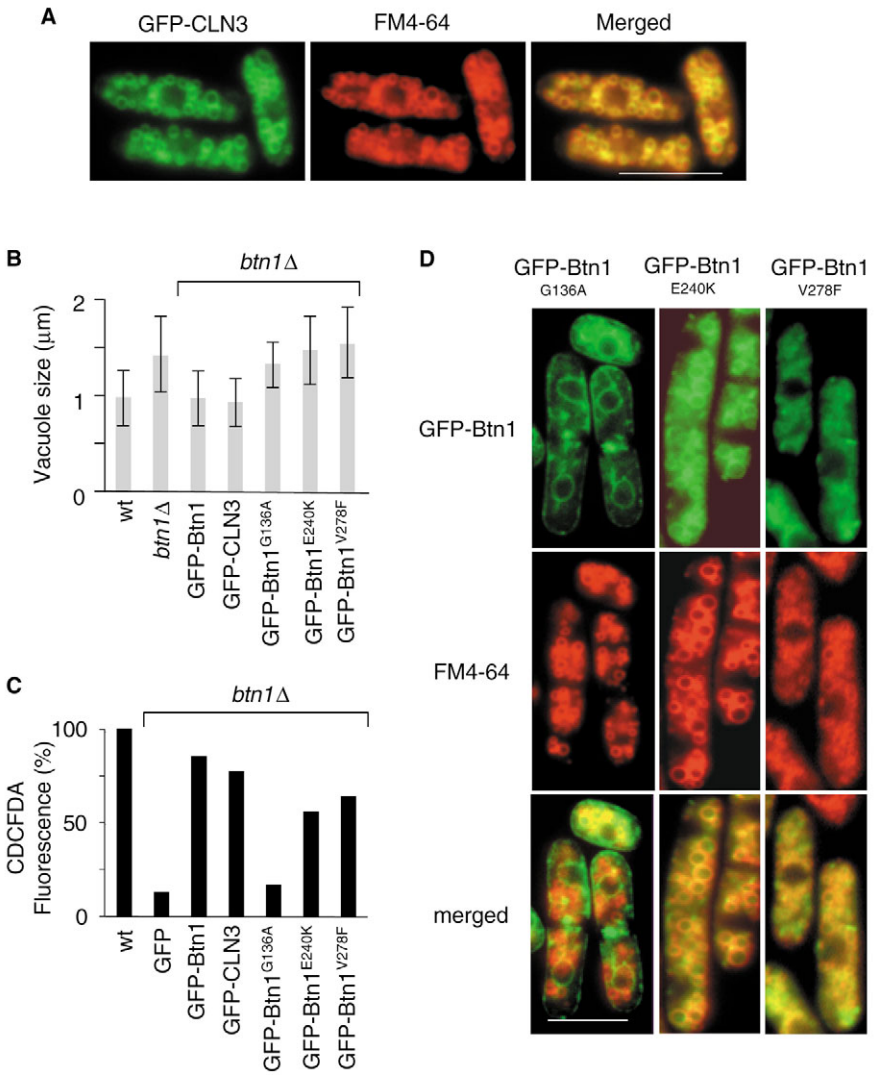


**Fig. 7.** Localisation and vacuolar effects of ectopically expressed CLN3 and Btn1p mutants. (A) Cells deleted for *btn1* and expressing human CLN3 protein (GFP-CLN3) for 18 hours (green, left panel) were labelled with FM4-64 (red, middle panel). CLN3 trafficked to the vacuole in *btn1Δ* cells, as can be seen in the merged images. Bar, 10 μm. (B) Vacuole size analysis of wild-type cells (wt), cells deleted for *btn1* (*btn1Δ*), and cells deleted for *btn1* and expressing wild-type (GFP-Btn1) protein or human CLN3 protein (GFP-CLN3), or cells deleted for *btn1* and expressing mutant Btn1 protein (GFP-Btn1$^{G136A}$, -Btn1$^{E240K}$ or -Btn1$^{V278F}$). The vacuoles of cells expressing the mutant proteins remained enlarged in contrast to those expressing wild-type Btn1 or CLN3 which were reduced in size. (C) CDCFDA fluorescence determined in wild-type cells (wt), in cells deleted for *btn1* and expressing GFP from vector alone (GFP), or wild-type Btn1 protein (GFP-Btn1) or human CLN3 protein (GFP-CLN3), or cells deleted for *btn1* and expressing mutant Btn1 protein (GFP-Btn1$^{G136A}$, -Btn1$^{E240K}$ or -Btn1$^{V278F}$). The vacuolar pH of cells expressing GFP-Btn1$^{G136A}$ was similar to that of *btn1Δ* cells. The vacuolar pH of cells expressing GFP-Btn1$^{E240K}$ and GFP-Btn1$^{V278F}$ was partially rescued. (D) Expression of GFP-Btn1 mutant protein (green, top panel) was repressed in cells deleted for *btn1* for 3 hours, then cells were labelled with FM4-64 (red, middle panel). GFP-Btn1$^{G136A}$ was retarded in the endoplasmic reticulum but GFP-Btn1$^{E240K}$ and GFP-Btn1$^{V278F}$ trafficked to the vacuolar membrane. Cells overexpressing GFP-Btn1$^{E240K}$ were also strikingly elongated. Bar, 5 μm.

## Btn1p acts in vacuole pH homeostasis

Two significant finding of these studies were that vacuolar pH was elevated by approximately 1 pH unit in *btn1Δ* cells and that overexpression of Btn1p reduced vacuole pH, strongly supporting a role for Btn1p in vacuole homeostasis. This is opposite to that reported for *btn1Δ* strains of budding yeast (Pearce, et al., 1998), and CLN3 overexpression studies in HEK293 cells (Golabek et al., 2000), but in agreement with observations made in cells from most types of NCL, including JNCL (Holopainen et al., 2001), supporting the use of fission yeast as a model for Batten disease. Our observation that the severity of mutations in Btn1p that mimicked those causing JNCL correlated with the increased vacuole pH further supports the use of fission yeast as a model for Batten disease.

## Btn1p is functional in a pre-vacuolar compartment

Trafficking of Btn1p to the vacuole appeared to follow or overlap with the endocytic route since it was first visible in early FM4-64-staining compartments and was dependent on Ypt7p, which is required for vacuole fusion (Bone et al., 1998). However, trafficking of Btn1p to the vacuole, like other vacuole membrane proteins, was not dependent on a functioning vATPase, required for acidification of the endocytic pathway and for endocytosis (Iwaki et al., 2004b), suggesting that an alternate route to the vacuole can be exploited. Vacuole size in *ypt7Δ* cells increased when *btn1* was also deleted, indicating that Btn1p exerted an effect on vacuole size separate from that within the vacuole membrane, i.e. it has a functional role in a pre-vacuolar compartment. Cells deleted for *vma1* required Btn1p for cytokinesis. This implies either that the non-vacuolar role of Btn1p is required for cytokinesis and is independent of its contribution to vacuole function or that the function of Btn1 in a vacuole lacking a functional vATPase is essential for cytokinesis.

## The disease severity of disease mutations may correlate with their effect on vacuole pH

Overexpression of three different disease-causing mutations in Btn1p in a *btn1* null background caused enlargement of vacuoles but had different effects on vacuolar pH. In humans, the CLN3 mutation G187A causes a classic disease course, and expression of GFP-Btn1$^{G136A}$ did not rescue the pH defect of

*btn1Δ* cells. Residue G187 (G136 in Btn1p) is located within a highly conserved stretch of amino acids that is predicted to project into the lumen of the organelle (Ezaki et al., 2003; Janes et al., 1996; Kyttälä et al., 2003; Mao et al., 2003). Its mutation could interfere with the conformation of Btn1p, consistent with its retarded trafficking and retention within the ER. Disease mutation E295K is associated with a markedly protracted disease course (Lauronen et al., 1999; Munroe et al., 1997; Wisniewski et al., 1998) suggesting that the mutant protein retains significant residual activity. Consistently, GFP-Btn1$^{E240K}$ protein targeted the vacuole membrane and partially rescued the vacuolar pH defect of *btn1Δ* cells, further supporting a link between disease severity and vacuole pH in this model system. The same mutant CLN3 protein trafficked to the lysosome (Järvelä et al., 1999). Mutation V330F, although thought to be associated with a classical disease course (Munroe et al., 1997), when expressed in *S. cerevisiae* clearly allowed residual activity of the mutant protein (Haskell et al., 2000), consistent with the ability of GFP-Btn1$^{V278F}$ to traffic to the vacuole and partially rescue the pH defect of *btn1Δ* cells. It has not been possible to confirm whether the patient originally reported as carrying the mutation V330F did indeed have a more protracted disease course. Mutant E295K was also associated with a marked increase in cell length, indicative of a significant delay in the cell cycle that must be connected with the residual Btn1p activity associated with this mutant, and may be linked to the requirement for Btn1p for cytokinesis in *vma1Δ* cells and the higher septation index and slower growth of *btn1Δ* cells.

## The molecular basis of NCL

How does absence or mutation in CLN3 cause disease? Our results are consistent with observations that the pH of lysosomes in cells from a JNCL patient are more alkaline. This would affect the activity of lysosomal enzymes and membrane transporters and may explain the accumulation of undegraded material as the disease progresses, with the build-up of subunit c of mitochondrial ATP synthase due to a defect in the final stages of autophagocytic degradation (Nakamura et al., 1997). In addition to other types of NCLs (Holopainen et al., 2001), another lysosomal storage disorder, mucolipidosis IV, is associated with enlarged lysosomes and increased lysosomal pH (Bach et al., 1999). The MCOLN1 gene encodes a transient receptor potential (TRP)-related channel that is pH regulated and involved in fusion of membranes within the endosome-lysosome system (LaPlante et al., 2004; Raychowdhury et al., 2004). Altered lysosomal pH might therefore exert a secondary effect on trafficking and fusion of compartments of the endocytic pathway and other vesicular routes. In *S. pombe*, we have also shown that in cells already compromised in the acidification of vesicular compartments (i.e. cells deleted for *vma1*) Btn1p is essential for septum formation (Wang, H. et al., 2002), and in cells lacking *btn1* the process of septation is lengthened. In the brain, a defect in trafficking could have a significant impact on transmitter movement, release and uptake and may be the molecular basis for the neurodegeneration that occurs in JNCL. However it is also possible that these effects are secondary to the loss of function of CLN3, and whilst they may contribute significantly to the disease mechanism, the primary function of CLN3 has yet to be defined.

Fission yeast lacking the *S. pombe* orthologue of another human NCL gene, *CLN1*, were also retarded in their growth and were sensitive to raised extracellular pH and to sodium orthovanadate (Cho et al., 2004). This implicates Ppt1p in activities that may affect vacuole pH or homeostasis. The severity of the sensitivity to raised extracellular pH was more marked in *S. pombe* cells expressing mutant Ppt1p than those with mutant Btn1p, in line with the severity of the human disease, and supports the hypothesis that part of the pathogenesis of NCL may be due to increased lysosomal pH. In *S. cerevisiae*, palmitoylation is known to be important in vacuole fusion (Dietrich et al., 2004; Wang, Y. et al., 2001) suggesting that depalmitoylation may also be important, either as a switch or during protein turnover. Thus inactivity of a depalmitoylating enzyme such as Ppt1p, or of the protein Btn1p, may interfere with vacuole integrity through defects in vacuole fusion and pH homeostasis. Just as the use of budding yeast is proving fruitful as a model for other neurodegenerative disorders (Malathi et al., 2004; Outeiro et al., 2004) we conclude that the use of fission yeast, with its many vacuoles, is particularly appropriate to model Batten disease, and the advantages associated with such a genetically tractable organism may prove vital in determining the function of Btn1p/CLN3 and the biological roles of both Btn1p/CLN3 and Ppt1/CLN1.

We thank Kaoru Takegawa and John Armstrong for supplying strains, and Chris Knapp and Vasanti Amin for excellent technical assistance. Y.G. and S.C. were supported by the Wellcome Trust, UK (grants 066043 to J.H. and 054606 to S.M.). We thank the Children's Brain Diseases Foundation, USA and the Batten Disease Support and Research Association, USA for additional financial support.

## References

**Alfa, C. E., Fantes, P., Hyams, J. S., McLeod, M. and Warbrick, E.** (1993). *Experiments with fission yeast: A laboratory course manual*. Cold Spring Harbor, NY: Cold Spring Harbor Press.

**Bach, G., Chen, C. S. and Pagano, R. E.** (1999). Elevated lysosomal pH in Mucolipidosis type IV cells. *Clin. Chim. Acta* **280**, 173-179.

**Bellemare, D. R., Shaner, L., Morano, K. A., Beaudoin, J., Langlois, R. and Labbe, S.** (2002). Ctr6, a vacuolar membrane copper transporter in Schizosaccharomyces pombe. *J. Biol. Chem.* **277**, 46676-46686.

**Bone, N., Millar, J. B., Toda, T. and Armstrong, J.** (1998). Regulated vacuole fusion and fission in *Schizosaccharomyces pombe*: an osmotic response dependent on MAP kinases. *Curr. Biol.* **8**, 135-144.

**Brazer, S. C., Williams, H. P., Chappell, T. G. and Cande, W. Z.** (2000). A fission yeast kinesin affects Golgi membrane recycling. *Yeast* **16**, 149-166.

**Chattopadhyay, S., Muzaffar, N. E., Sherman, F. and Pearce, D. A.** (2000). The yeast model for Batten disease: mutations in *BTN1*, *BTN2* and *HSP30* alter pH homeostasis. *J. Bacteriol.* **182**, 6418-6423.

**Cho, S. K. and Hofmann, S. L.** (2004). pdf1, a palmitoyl protein thioesterase 1 ortholog in *Schizosaccharomyces pombe*: a yeast model of infantile Batten disease. *Eukaryot. Cell* **3**, 302-310.

**Cousin, M. A. and Nicholls, D. G.** (1997). Synaptic vesicle recycling in cultured cerebellar granule cells: role of vesicular acidification and refilling. *J. Neurochem.* **69**, 1927-1935.

**Craven, R. A., Griffiths, D. J., Sheldrick, K. S., Randall, R. E., Hagan, I. M. and Carr, A. M.** (1998). Vectors for the expression of tagged proteins in Schizosaccharomyces pombe. *Gene* **221**, 59-68.

**Croopnick, J. B., Choi, H. C. and Mueller, D. M.** (1998). The subcellular location of the yeast *Saccharomyces cerevisiae* homologue of the protein defective in the juvenile form of Batten disease. *Biochem. Biophys. Res. Commun.* **250**, 335-341.

**Dietrich, L. E., Gurezka, R., Veit, M. and Ungermann, C.** (2004). The SNARE Ykt6 mediates protein palmitoylation during an early stage of homotypic vacuole fusion. *EMBO J.* **23**, 45-53.

**Ezaki, J., Takeda-Ezaki, M., Koike, M., Ohsawa, Y., Taka, H., Mineki, R.,**

**Murayama, K., Uchiyama, Y., Ueno, T. and Kominami, E.** (2003). Characterization of Cln3p, the gene product responsible for juvenile neuronal ceroid lipofuscinosis, as a lysosomal integral membrane glycoprotein. *J. Neurochem.* **87**, 1296-1308.

**Gachet, Y. and Hyams, J. S.** (2005). Endocytosis in fission yeast is spatially associated with the actin cytoskeleton during polarised growth and cytokinesis. *J. Cell Sci.* **118**, 4231-4242.

**Gaits, F. and Russell, P.** (1999). Vacuole fusion regulated by protein phosphatase 2C in fission yeast. *Mol. Biol. Cell* **10**, 2647-2654.

**Gao, H., Boustany, R. M., Espinola, J. A., Cotman, S. L., Srinidhi, L., Antonellis, K. A., Gillis, T., Qin, X., Liu, S., Donahue, L. R. et al.** (2002). Mutations in a novel CLN6-encoded transmembrane protein cause variant neuronal ceroid lipofuscinosis in man and mouse. *Am. J. Hum. Genet.* **70**, 324-335.

**Goebel, H. H., Mole, S. E. and Lake, B. D.** (1999). The neuronal ceroid lipofuscinoses (Batten disease). In *Biomedical and Health Research*, p. 211. Amsterdam: IOS Press.

**Golabek, A. A., Kida, E., Walus, M., Kaczmarski, W., Michalewski, M. and Wisniewski, K. E.** (2000). CLN3 protein regulates lysosomal pH and alters intracellular processing of Alzheimer's amyloid-beta protein precursor and cathepsin D in human cells. *Mol. Genet. Metab.* **70**, 203-213.

**Haskell, R. E., Carr, C. J., Pearce, D. A., Bennett, M. J. and Davidson, B. L.** (2000). Batten disease: evaluation of *CLN3* mutations on protein localization and function. *Hum. Mol. Genet.* **9**, 735-744.

**Heine, C., Koch, B., Storch, S., Kohlschutter, A., Palmer, D. N. and Braulke, T.** (2004). Defective ER-resident membrane protein CLN6 affects lysosomal degradation of endocytosed arylsulfatase A. *J. Biol. Chem.* **279**, 22347-22352.

**Holopainen, J. M., Saarikoski, J., Kinnunen, P. K. and Järvelä, I.** (2001). Elevated lysosomal pH in neuronal ceroid lipofuscinoses (NCLs). *Eur. J. Biochem.* **268**, 5851-5856.

**International Batten Disease Consortium, The** (1995). Isolation of a novel gene underlying Batten disease, *CLN3*. *Cell* **82**, 949-957.

**Isosomppi, J., Vesa, J., Jalanko, A. and Peltonen, L.** (2002). Lysosomal localization of the neuronal ceroid lipofuscinosis CLN5 protein. *Hum. Mol. Genet.* **11**, 885-891.

**Iwaki, T., Osawa, F., Onishi, M., Koga, T., Fujita, Y., Hosomi, A., Tanaka, N., Fukui, Y. and Takegawa, K.** (2003). Characterization of *vps33+*, a gene required for vacuolar biogenesis and protein sorting in *Schizosaccharomyces pombe*. *Yeast* **20**, 845-855.

**Iwaki, T., Goa, T., Tanaka, N. and Takegawa, K.** (2004a). Characterization of *Schizosaccharomyces pombe* mutants defective in vacuolar acidification and protein sorting. *Mol. Genet. Genomics* **271**, 197-207.

**Iwaki, T., Tanaka, N., Takagi, H., Giga-Hama, Y. and Takegawa, K.** (2004b). Characterization of *end4+*, a gene required for endocytosis in *Schizosaccharomyces pombe*. *Yeast* **21**, 867-881.

**Janes, R. W., Munroe, P. B., Mitchsion, H. M., Gardiner, R. M., Mole, S. E. and Wallace, B. A.** (1996). A model for Batten disease protein CLN3: Functional implications from homology and mutations. *FEBS Lett.* **399**, 75-77.

**Järvelä, I., Sainio, M., Rantamaki, T., Olkkonen, V. M., Carpén, O., Peltonen, L. and Jalanko, A.** (1998). Biosynthesis and intracellular targeting of the CLN3 protein defective in Batten disease. *Hum. Mol. Genet.* **7**, 85-90.

**Järvelä, I., Lehtovirta, M., Tikkanen, R., Kyttälä, A. and Jalanko, A.** (1999). Defective intracellular transport of CLN3 is the molecular basis of Batten disease (JNCL). *Hum. Mol. Genet.* **8**, 1091-1098.

**Kaczmarski, W., Wisniewski, K. E., Golabek, A., Kaczmarski, A., Kida, E. and Michalewski, M.** (1999). Studies of membrane association of CLN3 protein. *Mol. Genet. Metab.* **66**, 261-264.

**Kim, Y., Ramirez-Montealegre, D. and Pearce, D. A.** (2003). A role in vacuolar arginine transport for yeast Btn1p and for human CLN3, the protein defective in Batten disease. *Proc. Natl. Acad. Sci. USA* **100**, 15458-15462.

**Korey, C. A. and MacDonald, M. E.** (2003). An over-expression system for characterizing Ppt1 function in *Drosophila*. *BMC Neurosci.* **4**, 30.

**Kyttälä, A., Ihrke, G., Vesa, J., Schell, M. J. and Luzio, J. P.** (2003). Two motifs target Batten disease protein CLN3 to lysosomes in transfected non-neuronal and neuronal cells. *Mol. Biol. Cell*. **15,** 1313-1323.

**Kyttälä, A., Yliannala, K., Schu, P., Jalanko, A. and Luzio, J. P.** (2005). AP-1 and AP-3 facilitate lysosomal targeting of Batten disease protein CLN3 via its dileucine motif. *J. Biol. Chem.* **280**, 10277-10283.

**LaPlante, J. M., Ye, C. P., Quinn, S. J., Goldin, E., Brown, E. M., Slaugenhaupt, S. A. and Vassilev, P. M.** (2004). Functional links between mucolipin-1 and Ca2+-dependent membrane trafficking in mucolipidosis IV. *Biochem. Biophys. Res. Commun.* **322**, 1384-1391.

**Lauronen, L., Munroe, P. B., Järvelä, I., Autti, T., Mitchison, H. M., O'Rawe, A. M., Gardiner, R. M., Mole, S. E., Puranen, J., Häkkinen, A.-M. et al.** (1999). Delayed classic and protracted phenotypes of compound heterozygous juvenile neuronal ceroid lipofuscinosis. *Neurology* **52**, 360-365.

**Li, Y. C., Chen, C. R. and Chang, E. C.** (2000). Fission yeast Ras1 effector Scd1 interacts with the spindle and affects its proper formation. *Genetics* **156**, 995-1004.

**Lonka, L., Kyttälä, A., Ranta, S., Jalanko, A. and Lehesjoki, A. E.** (2000). The neuronal ceroid lipofuscinosis CLN8 membrane protein is a resident of the endoplasmic reticulum. *Hum. Mol. Genet.* **9**, 1691-1697.

**Lonka, L., Salonen, T., Siintola, E., Kopra, O., Lehesjoki, A. E. and Jalanko, A.** (2004). Localization of wild-type and mutant neuronal ceroid lipofuscinosis CLN8 proteins in non-neuronal and neuronal cells. *J. Neurosci. Res.* **76**, 862-871.

**Luiro, K., Kopra, O., Lehtovirta, M. and Jalanko, A.** (2001). CLN3 protein is targeted to neuronal synapses but excluded from synaptic vesicles: new clues to Batten disease. *Hum. Mol. Genet.* **10**, 2123-2131.

**Malathi, K., Higaki, K., Tinkelenberg, A. H., Balderes, D. A., Almanzar-Paramio, D., Wilcox, L. J., Erdeniz, N., Redican, F., Padamsee, M., Liu, Y. et al.** (2004). Mutagenesis of the putative sterol-sensing domain of yeast Niemann Pick C-related protein reveals a primordial role in subcellular sphingolipid distribution. *J. Cell Biol.* **164**, 547-556.

**Mao, Q., Foster, B. J., Xia, H. and Davidson, B. L.** (2003). Membrane topology of CLN3, the protein underlying Batten disease. *FEBS Lett.* **541**, 40-46.

**Maundrell, K.** (1993). Thiamine-repressible expression vectors pREP and pRIP for fission yeast. *Gene* **123**, 127-130.

**Mellman, I., Fuchs, R. and Helenius, A.** (1986). Acidification of the endocytic and exocytic pathways. *Annu. Rev. Biochem.* **55**, 663-700.

**Michalewski, M. P., Kaczmarski, W., Golabek, A. A., Kida, E., Kaczmarski, A. and Wisniewski, K. E.** (1998). Evidence for phosphorylation of CLN3 protein associated with Batten disease. *Biochem. Biophys. Res. Commun.* **253**, 458-462.

**Michalewski, M. P., Kaczmarski, W., Golabek, A. A., Kida, E., Kaczmarski, A. and Wisniewski, K. E.** (1999). Posttranslational modification of CLN3 protein and its possible functional implication. *Mol. Genet. Metab.* **66**, 272-276.

**Mitchell, W. A., Porter, M., Kuwabara, P. and Mole, S. E.** (2001). Genomic structure of three *CLN3*-like genes in *Caenorhabditis elegans*. *Eur. J. Paediatr. Neurol.* **5**, 121-126.

**Mole, S. E., Michaux, G., Codlin, S., Wheeler, R. B., Sharp, J. D. and Cutler, D. F.** (2004). CLN6, which is associated with a lysosomal storage disease, is an endoplasmic reticulum protein. *Exp. Cell Res.* **298**, 399-406.

**Moreno, S., Klar, A. and Nurse, P.** (1991). Molecular genetic analysis of fission yeast *Schizosaccharomyces pombe*. *Methods Enzymol.* **194**, 795-823.

**Munroe, P. B., Mitchison, H. M., O'Rawe, A. M., Anderson, J. W., Boustany, R.-M., Lerner, T. J., Taschner, P. E. M., de Vos, N., Breuning, M. H., Gardiner, R. M. et al.** (1997). Spectrum of mutations in the Batten disease gene, *CLN3*. *Am. J. Hum. Genet.* **61**, 310-316.

**Murray, J. M. and Johnson, D. I.** (2001). The Cdc42p GTPase and its regulators Nrf1p and Scd1p are involved in endocytic trafficking in the fission yeast *Schizosaccharomyces pombe*. *J. Biol. Chem.* **276**, 3004-3009.

**Nakamura, N., Matsuura, A., Wada, Y. and Ohsumi, Y.** (1997). Acidification of vacuoles is required for autophagic degradation in the yeast, Saccharomyces cerevisiae. *J. Biochem. (Tokyo)* **121**, 338-344.

**Outeiro, T. F. and Muchowski, P. J.** (2004). Molecular genetics approaches in yeast to study amyloid diseases. *J. Mol. Neurosci.* **23**, 49-60.

**Pearce, D. A. and Sherman, F.** (1997). BTN1, a yeast gene corresponding to the human gene responsible for Batten's disease, is not essential for viability, mitochondrial function, or degradation of mitochondrial ATP synthase. *Yeast* **13**, 691-697.

**Pearce, D. A. and Sherman, F.** (1998). A yeast model for the study of Batten disease. *Proc. Natl. Acad. Sci. USA* **95**, 6915-6918.

**Pearce, D. A., Carr, C. J., Das, B. and Sherman, F.** (1999a). Phenotypic reversal of the btn1 defects in yeast by chloroquine: a yeast model for Batten disease. *Proc. Natl. Acad. Sci. USA* **96**, 11341-11345.

**Pearce, D. A., Ferea, T., Nosel, S. A., Das, B. and Sherman, F.** (1999b). Action of *BTN1*, the yeast orthologue of the gene mutated in Batten disease. *Nat. Genet.* **22**, 55-58.

**Pidoux, A. L. and Armstrong, J.** (1993). The BiP protein and the

endoplasmic reticulum of Schizosaccharomyces pombe: fate of the nuclear envelope during cell division. *J. Cell Sci.* **105**, 1115-1120.

**Porter, M. Y., Turmaine, M. and Mole, S. E.** (2005). Identification and characterization of *Caenorhabditis elegans* palmitoyl protein thioesterase-1. *J. Neurosci. Res.* **79**, 836-848.

**Pringle, J. R., Preston, R. A., Adams, A. E., Stearns, T., Drubin, D. G., Haarer, B. K. and Jones, E. W.** (1989). Fluorescence microscopy methods for yeast. *Methods Cell Biol.* **31**, 357-435.

**Pullarkat, R. K. and Morris, G. N.** (1997). Farnesylation of Batten disease CLN3 protein. *Neuroped.* **28**, 42-44.

**Ranta, S., Zhang, Y., Ross, B., Lonka, L., Takkunen, E., Messer, A., Sharp, J., Wheeler, R., Kusumi, K., Mole, S. et al.** (1999). The neuronal ceroid lipofuscinoses in human EPMR and *mnd* mutant mice are associated with mutations in *CLN8*. *Nat. Genet.* **23**, 233-236.

**Ranta, S., Topçu, M., Tegelberg, S., Tan, H., Üstübütün, A., Saatci, I., Dufke, A., Enders, H., Pohl, K., Alembik, Y. et al.** (2004). Variant late infantile neuronal ceroid lipofuscinosis in a subset of Turkish patients is allelic to Northern epilepsy. *Hum. Mutat.* **23**, 300-305.

**Raychowdhury, M. K., Gonzalez-Perrett, S., Montalbetti, N., Timpanaro, G. A., Chasan, B., Goldmann, W. H., Stahl, S., Cooney, A., Goldin, E. and Cantiello, H. F.** (2004). Molecular pathophysiology of mucolipidosis type IV: pH dysregulation of the mucolipin-1 cation channel. *Hum. Mol. Genet.* **13**, 617-627.

**Santavuori, P.** (1988). Neuronal ceroid lipofuscinosis in childhood. *Brain Dev.* **10**, 80-83.

**Savukoski, M., Klockars, T., Holmberg, V., Santavuori, P., Lander, E. S. and Peltonen, L.** (1998). *CLN5*, a novel gene encoding a putative transmembrane protein mutated in Finnish variant late infantile neuronal ceroid lipofuscinosis. *Nat. Genet.* **19**, 286-288.

**Seeley, E. S., Kato, M., Margolis, N., Wickner, W. and Eitzen, G.** (2002). Genomic analysis of homotypic vacuole fusion. *Mol. Biol. Cell* **13**, 782-794.

**Sleat, D. E., Donnelly, R. J., Lackland, H., Liu, C.-G., Sohar, I., Pullarkat, R. K. and Lobel, P.** (1997). Association of mutations in a lysosomal protein with classical late-infantile neuronal ceroid lipofuscinosis. *Science* **277**, 1802-1805.

**Storch, S., Pohl, S. and Braulke, T.** (2004). A dileucine motif and a cluster of acidic amino acids in the second cytoplasmic domain of the Batten disease-related CLN3 protein are required for efficient lysosomal targeting. *J. Biol. Chem.* **279**, 53625-53634.

**Takegawa, K., Iwaki, T., Fujita, Y., Morita, T., Hosomi, A. and Tanaka, N.** (2003). Vesicle-mediated protein transport pathways to the vacuole in *Schizosaccharomyces pombe*. *Cell Struct. Funct.* **28**, 399-417.

**Vesa, J., Hellsten, E., Verkruyse, L. A., Camp, L. A., Rapola, J., Santavuori, P., Hofmann, S. L. and Peltonen, L.** (1995). Mutations in the palmitoyl protein thioesterase gene causing infantile neuronal ceroid lipofuscinosis. *Nature* **376**, 584-587.

**Vines, D. J. and Warburton, M. J.** (1999). Classical late infantile neuronal ceroid lipofuscinosis fibroblasts are deficient in lysosomal tripeptidyl peptidase I. *FEBS Lett.* **443**, 131-135.

**Wang, H., Tang, X., Liu, J., Trautmann, S., Balasundaram, D., McCollum, D. and Balasubramanian, M. K.** (2002). The multiprotein exocyst complex is essential for cell separation in *Schizosaccharomyces pombe*. *Mol. Biol. Cell* **13**, 515-529.

**Wang, Y. X., Kauffman, E. J., Duex, J. E. and Weisman, L. S.** (2001). Fusion of docked membranes requires the armadillo repeat protein Vac8p. *J. Biol. Chem.* **276**, 35133-35140.

**Wheeler, R. B., Sharp, J. D., Schultz, R. A., Joslin, J. M., Williams, R. E. and Mole, S. E.** (2002). The gene mutated in variant late infantile neuronal ceroid lipofuscinosis (*CLN6*) and *nclf* mutant mice encodes a novel predicted transmembrane protein. *Am. J. Hum. Genet.* **70**, 537-542.

**Wickner, W.** (2002). Yeast vacuoles and membrane fusion pathways. *EMBO J.* **21**, 1241-1247.

**Wisniewski, K. E., Zhong, N., Kaczmarski, W., Kaczmarski, A., Kida, E., Brown, W. T., Schwarz, K. O., Lazzarini, A. M., Rubin, A. J., Stenroos, E. S. et al.** (1998). Compound heterozygous genotype is associated with protracted juvenile neuronal ceroid lipofuscinosis. *Ann. Neurol.* **43**, 106-110.